

17. B. Averboukh, R. Huber, K. W. Cheah, Y. R. Shen, G. G. Qin, Z. C. Ma, and W. H. Zong, "Luminescence studies of a Si/SiO₂ superlattice," *J. Appl. Phys.* **92**(7), 3564–3568 (2002).
18. M. Sykora, L. Mangolini, R. D. Schaller, U. Kortshagen, D. Jurbergs, and V. I. Klimov, "Size-dependent intrinsic radiative decay rates of silicon nanocrystals at large confinement energies," *Phys. Rev. Lett.* **100**(6), 067401 (2008).
19. S. Godefroo, M. Hayne, M. Jivanescu, A. Stesmans, M. Zacharias, O. I. Lebedev, G. Van Tendeloo, and V. V. Moshchalkov, "Classification and control of the origin of photoluminescence from Si nanocrystals," *Nat. Nanotechnol.* **3**(3), 174–178 (2008).
20. K. Dohnalová, K. Kůsová, and I. Pelant, "Time-resolved photoluminescence spectroscopy of the initial oxidation stage of small silicon nanocrystals," *Appl. Phys. Lett.* **94**(21), 211903 (2009).
21. J. Valenta, A. Fučíková, F. Vácha, F. Adamec, J. Humpolíčková, M. Hof, I. Pelant, K. Kůsová, K. Dohnalová, and J. Linnros, "Light-emission performance of silicon nanocrystals deduced from single quantum dot spectroscopy," *Adv. Funct. Mater.* **18**(18), 2666–2672 (2008).
22. H. S. Jang, H. Yang, S. W. Kim, J. Y. Han, S.-G. Lee, and D. Y. Jeon, "White light-emitting diodes with excellent color rendering based on organically capped CdSe quantum dots and Sr₂SiO₅:Ce³⁺,Li⁺ phosphors," *Adv. Mater.* **20**(14), 2696–2702 (2008).
23. J. Ziegler, S. Xu, E. Kucur, F. Meister, M. Batentschuk, F. Gindele, and T. Nann, "Silica-coated InP/ZnS nanocrystals as converter material in white LEDs," *Adv. Mater.* **20**(21), 4068–4073 (2008).

1. Introduction

Solid-state lighting based on light-emitting diodes (LEDs) has been rapidly growing in recent years. Compared to conventional general illumination solutions such as incandescent bulbs and compact fluorescent lamps, the white LEDs have several advantages, including high luminous efficacy ($> 70 \text{ lm W}^{-1}$), long lifetimes ($> 25,000$ hours), dimmability, fast response times, and more. In most lighting applications which require the faithful reproduction of colors on objects, warm white light resembling incandescent light is usually desirable. Specifically, a light source with correlated color temperature (CCT) = 2700 to 3000 K and color rendering index (CRI) > 80 is able to produce the demanded lighting quality. Generally, the white LEDs achieve this standard by adding red-emitting Eu-doped phosphors, such as CaAlSiN₃:Eu (CASN) or CaS:Eu, to the yellow-emitting Y₃Al₅O₁₂:Ce³⁺ (YAG:Ce) phosphor which is pumped by blue LEDs. However, in the current LED phosphor market, the red-emitting Eu-doped phosphors are usually two to three times more expensive than the yellow-emitting YAG:Ce phosphors, which significantly increases the cost of high-CRI warm white LEDs. Besides, the supply of rare earth elements (REEs) in general has become unstable in recent years. For example, the price of europium oxide, which is the activating raw material of the Eu-doped phosphors, has increased by more than two times since early 2010 due to unstable supplies and increasing demand [1]. Furthermore, the extraction and processing of REEs is an environmental hazard due to open-pit mining and the natural inclusion of radioactive substances in REE-bearing ores. In recent years, semiconductor quantum dot (QD) phosphors have been considered promising substitutes for their REE counterparts in lighting applications because of their high photoluminescence quantum yield (PLQY), high color purity, tunable bandgap and broadband absorption [2]. For examples, green- and red-emitting CdSe QDs were hybridized on blue InGaN LEDs to achieve white light with CRI > 80 [3, 4]. However, the risk of cadmium-related cytotoxicity from these widely used CdSe QDs [5] and the use of the hot-injection method for their synthesis, which is relatively hard to scale up, are the two major barriers impeding their widespread commercialization.

In this paper, we demonstrate red-emitting phosphors based on silicon quantum dots (SiQDs) as a low-cost and environment-friendly alternative to the red-emitting Eu-doped phosphors or CdSe QDs. After passivation with silicon oxide and alkyl silanes, the red-emitting SiQD-phosphors have high PLQY = 51% with 365-nm excitation, which is comparable to the quantum efficiencies achieved by other direct bandgap semiconductor QDs. The red phosphors also have a peak photoluminescence (PL) wavelength at 630 nm and a full-width-at-half-maximum (FWHM) of 145 nm. The deep red emission, although relatively broadband compared to CdSe QDs which usually have FWHM < 50 nm, is ideal for forming the basis of a warm white spectrum. With UV (365 nm) or near-UV (405 nm) LED pumping

and the addition of some green- and/or blue-emitting REE phosphors, warm white LEDs with excellent color rendering capability have been achieved. Noticeably, fluorescent SiC is also an alternative to the current REE phosphors [6]. In addition to the phosphor application, SiQDs as efficient electroluminescent materials in LEDs have been demonstrated [7].

2. Experiment

We synthesized the red-emitting SiQD-phosphors in three major steps. Firstly, a 6-inch p-type silicon wafer was electrochemically etched in the electrolyte comprising HF and methanol, and the resulting porous silicon layer was mechanically harvested from the wafer surface [8–10]. Secondly, the silicon powders were collected, sonicated and dispersed in a mixture of HNO₃ and diluted HF for isotropic etching, followed by HNO₃ etching for passivating the silicon powders with a silicon oxide layer. Finally, the silicon powders were refluxed in 185 mM diphenylsilanediol in ethanol, followed by surface treatment with chlorotrimethylsilane in toluene. Generally, about 100 mg of phosphors was obtained per wafer per synthesis, and the concentration of about 2.5 mg mL⁻¹ in toluene was used for all optical characterizations. The PL and excitation spectra were measured using a Jobin Yvon Horiba Fluorolog FL-3 fluorometer system. The PLQYs were measured using a HAMAMATSU External Quantum Efficiency Measurement System (C9920) with quartz cuvettes. The absorbance spectra were measured using an Agilent 8453 Diode Array UV-Vis Spectrophotometer. The FTIR-ATR spectra were recorded using a Perkin Elmer FTIR Spectrum RX I system. The PL lifetimes were measured using a PicoQuant Time-Correlated Single Photon Counting System.

3. Results and discussion

The SiQD-phosphors have a unique structure, including a micron-size silicon core with nano-size SiQDs attached on the surface, as a result of the electrochemical etching process. The SEM image of the SiQD-phosphors is shown in Figs. 1(a) and 1(b) in low and high magnification, respectively. The silicon cores are mostly in sizes ranging from 1 to 5 μm, and each silicon core is covered with a nano-porous surface which is composed of wires of SiQDs of sizes around 5 nm as shown in the TEM image in Fig. 1(c). The SiQD size here is slightly bigger than the previous results obtained from bare porous silicon surface [11], likely due to the additional silicon oxide capping resulting from the HNO₃ etching step.

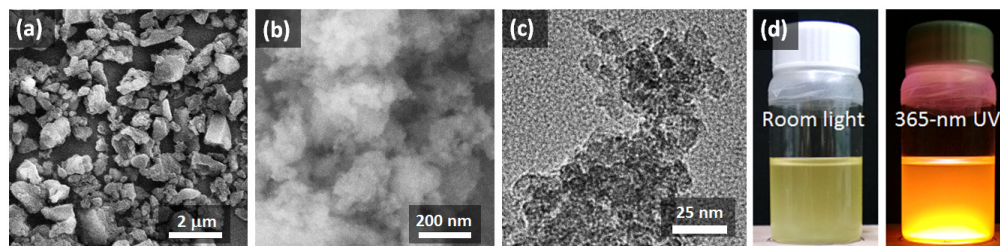


Fig. 1. (a) and (b) SEM images of the SiQD phosphors. (c) TEM image of the SiQD-phosphors. (d) Photographs of the SiQD-phosphor suspension in toluene under room light (left) and 365-nm near-UV excitation (right).

The photographs and PL spectra of the red-emitting SiQD-phosphor suspension in toluene are shown in Fig. 1(d) and Fig. 2(a), respectively. Despite different excitation wavelengths, the PL spectra have almost the same peak wavelengths at about 630 nm and FWHM of about 145 nm. The PLQY, measured by the integrating sphere method, of the same phosphor suspension as a function of excitation photon energy ranging from 2.70 eV (460 nm) to 4.13 eV (300 nm) is shown in Fig. 2(b). Particularly, the PLQY readings at 365 nm, 405 nm and 460 nm, the emission wavelengths of GaN or InGaN LEDs, are equal to 51%, 41% and 37%, respectively. In general, when the excitation photon energy increases, the PLQY of molecules or quantum dots is expected to remain constant (Kasha-Vavilov rule) or decrease as a result of

new non-radiative channels being activated [12]. In contrast, the PLQY of the SiQD-phosphors is higher at higher excitation energies. Previously, an analogous trend of PLQY increase was observed for porous silicon grain suspension in ethanol, made by a similar electrochemical etching method [13]. The enhancement of PLQY was attributed to carrier multiplication, where the excess energy of an excitation photon overcomes the threshold of a multiple of the band gap energy to produce an additional electron-hole pair, leading to more chances of radiative recombination and higher PLQY [13]. The PL spectrum of the SiQD-phosphors with its energy axis multiplied by two is placed at the bottom of Fig. 2(b), to show that the increase of PLQY starts to become obvious when the excitation photon energy is about two times of the SiQD band gap energy. Moreover, since the non-radiative microns-size cores are also present in the integrating sphere when measuring PLQY, the PL photons emitted by the SiQDs can potentially be re-absorbed by the cores which have a small energy band gap (1.11eV) of bulk silicon. Therefore, the actual PLQY without the re-absorption effect should be higher than the measured values in Fig. 2(b).

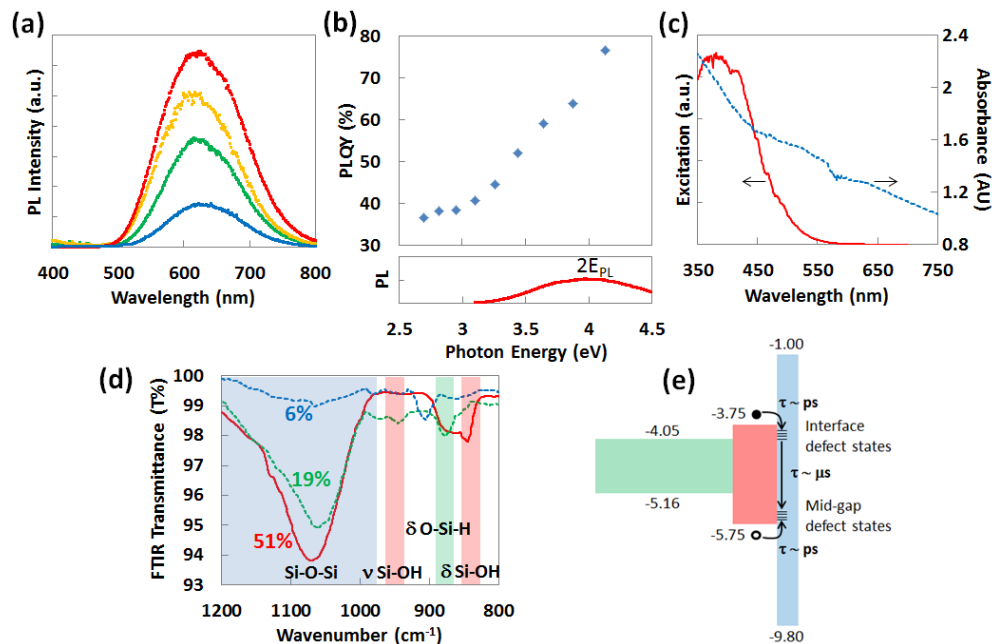


Fig. 2. (a) PL spectra of the SiQD-phosphor suspension in toluene, with 320-nm (orange curve), 365-nm (red curve), 400-nm (green curve) and 440-nm (blue curve) excitations, respectively. (b) PLQY versus excitation photon energy. (c) Excitation (red solid line) and absorbance (blue dotted line) spectra. (d) FTIR-ATR spectra of the dried SiQD-phosphor powders at different stages of the synthesis, as-harvested (blue dotted line), after HNO_3 etching (green dotted line) and after alkyl silane treatment (red solid line). ν and δ mean stretching mode and deformation mode, respectively. (e) Electronic band structure of the SiQD-phosphors. The green, red, blue rectangles represent the energy band gaps of the silicon core, SiQD and silicon oxide, respectively.

The excitation spectrum of the red-emitting SiQD-phosphor suspension is shown in Fig. 2(c). During the excitation measurement, the PL intensity at 630 nm reached its maximum when the excitation was at around 375 nm. At 405-nm and 450-nm excitation, the PL intensity was 90% and 55% of the maximum, respectively. The absorbance (or extinction) has a much broader spectrum than the excitation, due to a combination of scattering and absorption effects by the micron-size cores [14]. Especially at wavelengths longer than 550 nm, the absorbance of the phosphor suspension simply does not contribute to PL. Previously, single luminescent porous silicon nanoparticles which do not have the micron-size cores were

estimated to have PLQY as high as 88% [15]. Therefore, to further improve PLQY, decreasing the proportion of non-radiative bulk silicon in the SiQD-phosphors is critical. Noticeably, PLQY > 60% of SiQDs measured with 380-nm LED excitation in an integrating sphere has been achieved [16]. However, the PL wavelengths of these SiQDs are within the near-IR range, and hence are not suitable for lighting applications which require high spectral efficiencies, i.e. high luminous efficacy of optical radiation ($\text{LER, lm W}_{\text{opt}}^{-1}$).

The FTIR transmittance spectra of the red-emitting SiQD-phosphors measured by attenuated total reflectance (ATR) technique are shown in Fig. 2(d), in which different lines represent the spectra taken at different stages of the synthesis process. The silicon powders which have just been harvested from the silicon wafer after electrochemical etching have weak Si–O–Si absorption (975 to 1200 cm^{-1}), and the PLQY is as low as 6%. After HNO_3 etching, the Si–O–Si absorption compared to other bonds become stronger, and the PLQY improves to 19%. The final alkyl silane treatment leads to the most improvement of the PLQY to 51%, while the absorption of Si–O–Si, δ O–Si–H (875 cm^{-1}) and δ Si–OH (833 cm^{-1}) also shows significant enhancement correspondingly. Therefore, the surface passivating chemistry which involves various silicon-oxygen bonds, especially Si–O–Si, and the quality of passivation are closely related to the PLQY performance. All PLQY values in Fig. 2(d) are measured with 365-nm excitation, and toluene as the suspending solvent.

We also measured the PL lifetime of the red-emitting SiQD-phosphor suspension by using a time-correlated single photon counting technique. Unlike conventional CdSe QDs with short PL lifetime in nanoseconds, the SiQD-phosphors have a PL lifetime likely greater than 100 μs with no obvious fast decay component. Based on the long PL lifetime, the relatively broadband PL (FWHM = 145 nm) and the insensitivity of the PL peak wavelength to the excitation photon energies [Fig. 2(a)], we conclude that almost all radiative recombination happens between groups of oxide-related defect states, such as non-bridging oxygen-hole center (NBOHC), with little contribution from direct band-to-band transitions [17–19]. These radiative defect states, which are close to the band edges of SiQDs, even follow the band gap widening induced by the quantum confinement effect [8, 19]. As illustrated in Fig. 2(e), the PL process is initiated by absorption and inter-band carrier excitations in the SiQDs. Subsequently, the photo-excited carriers fast ($\tau \sim \text{ps}$) relax to the Si/SiO₂ interfacial defect states, and then slowly ($\tau \sim \mu\text{s}$) recombine while emitting broadband PL photons [20]. It is worth mentioning that the long PL lifetime is not beneficial for lighting applications. Under strong illumination, the SiQDs with long PL lifetime might easily enter a multi-exciton regime in which the blinking effect as a result of the Auger-type recombination process will lower the average PLQY [21]. We are now in the process of characterizing the PLQY degradation induced by thermal and/or strong illumination. Our preliminary results suggest that the SiQD-phosphors have a reasonably good thermal stability. However, under extended strong illumination, the blinking effect and the formation of non-radiative defects, such as $P_{\text{b}(0)}$, $P_{\text{b}1}$, EX and E_{γ} [19], might lower the PLQY by a factor of 10% to 40%, depending on the chemistry and quality of the surface passivation of each SiQD-phosphor sample.

Here we demonstrate warm white LEDs based on the red-emitting SiQD-phosphors, with the addition of green-emitting REE phosphors (Eu-doped silicates, G1758TM purchased from Intematix) and blue-emitting REE phosphors (BaMgAl₁₀O₁₇:Eu, purchased from HEFA Rare Earth Canada Co. Ltd). The red-, green- and blue-emitting phosphors have their PL peak wavelengths at 630 nm, 507 nm and 450 nm, respectively. A light-converting film comprising the phosphors is separated from the LED chips by a light mixing chamber to mimic a remote-phosphor configuration, by which the phosphors endure less heat and illumination intensity for higher stability. An optical fiber tip collects the light passing through the light-converting film for spectral analysis by a spectrometer composed of a monochromator and a photonmultiplier tube (PMT). For Sample 1 with 405-nm excitation, the polystyrene light-converting film is homogeneously dispersed with the red and green phosphors. For Sample 2 with 365-nm excitation, the light-converting film is made from silicone encapsulant and the

red, green and blue phosphors are uniformly dispersed within. The electroluminescence spectra of Sample 1 and Sample 2 are shown in Figs. 3(a) and 3(b), respectively, and an ideal incandescent spectrum is superimposed for comparison. Figure 3(c) summarizes the specifications of the lighting quality produced by Sample 1, Sample 2 and the ideal incandescent source. Warm white LEDs of color rendering close to incandescent bulbs, CCT ~ 2800 K and CRI ~ 95 , have been achieved by using the relatively broadband red emission from the SiQD-phosphors as the foundational spectrum. The narrowband green and/or blue emission from REE phosphors compensates for spectral deficiencies in the shorter wavelengths. If only the red-emitting SiQD-phosphors were used, results of CCT = 1958 K and CRI = 68 were obtained. In the previous studies, other types of semiconductor QDs, such as CdSe or InP/ZnS QDs, have been used to compensate the deficiency in reds of REE phosphors, such as YAG:Ce, as opposed to our experiments where the red-emitting SiQDs are used as the primary phosphors. In their studies, the REE-QD hybrid configuration achieved CRI = 85 ~ 90 [22, 23].

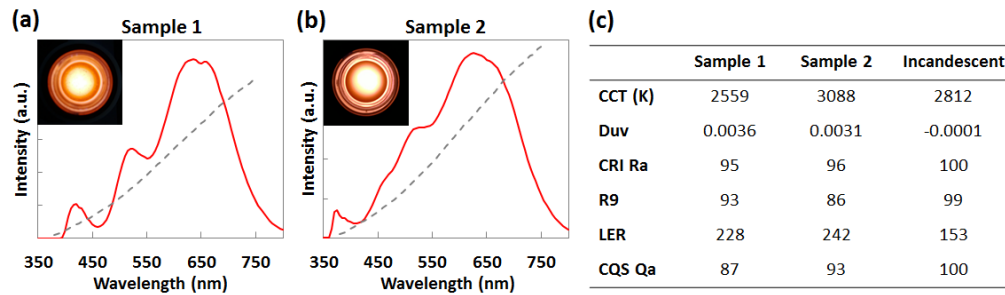


Fig. 3. (a) and (b) Electroluminescence spectra (area-normalized) and photographs of Sample 1 and Sample 2, respectively. The spectrum of an ideal incandescent source (gray dashed line) is superimposed for comparison. (c) Specifications of the lighting quality produced by Sample 1, Sample 2 and the ideal incandescent source. Duv specifies the deviation of a light from a blackbody radiator reference. R9 reports the rendering score of a light on a saturated red reference. LER ($\ln W_{\text{opt}}^{-1}$) represents the spectral efficiency. CQS Qa is a metric introduced by researchers at the National Institute of Science and Technology (NIST) as an update from the CRI standard.

4. Conclusion

The red-emitting SiQD-phosphors are used in warm white LEDs to achieve lighting quality (CCT ~ 2800 K and CRI ~ 95) close to an ideal incandescent light source. After surface passivation with silicon oxide and alkyl silanes, the phosphors have high PLQY equal to 51% and 41%, with 365-nm and 405-nm excitation, respectively. The PLQY of the SiQD-phosphors also increases as the excitation photon energy increases, likely due to the carrier multiplication effect. Based on the long PL lifetime, the relatively broadband PL and the insensitivity of the PL peak wavelength to the excitation photon energies, we conclude that almost all radiative recombination happens between groups of oxide-related defect states, with little contribution from quantum-confined band-to-band transitions. The SiQD-phosphors can potentially achieve higher PLQY by the removal of non-radiative bulk silicon currently present in the phosphors.

Acknowledgments

The authors thank NSF SBIR program, Washington Research Foundation, the W Fund, and Center for Commercialization (C4C) and Buerk Center for Entrepreneurship of the University of Washington for their funding support.